Available online at www.derpharmachemica.com

ISSN 0975-413X
CODEN (USA): PCHHAX

Der Pharma Chemica, 2016, 8(20):234-239
(http://derpharmachemica.com/archive.html)

Quantum Chemical Analysis of the Relationships between Electronic Structure and Antiviral Activity against HIV-1 of some Pyrazine-1,3-thiazine Hybrid Analogues

Juan S. Gómez-Jeria[1]*, Pablo Castro-Latorre[1] and Gaston A. Kpotin[2]

Quantum Pharmacology Unit, Department of Chemistry, Faculty of Sciences, University of Chile. Las Palmeras 3425, Santiago 7800003, Chile
Laboratory of Theoretical Chemistry and Molecular Spectroscopy, Faculty of Sciences and Technique, University of Abomey-Calavi, 03 BP 3409 Cotonou-Benin

---

ABSTRACT

We present the results of an analysis of the relationships between the electronic structure and the HIV-1 inhibition by a group of pyrazine-1,3-thiazine hybrid analogues. The electronic structure of all molecules was calculated within the Density Functional Theory at the B3LYP/6-31g(d,p) level with full geometry optimization. Linear multiple regression analysis techniques were employed to find the best relationship between inhibitory capacity and local atomic reactivity indices belonging to a common skeleton. We found statistically significant results. The corresponding partial inhibition pharmacophore suggest several atomic places to be employed for substitutions. The inhibition process seems to be mainly orbital-controlled.

Keywords: HIV-1, QSAR, DFT, electronic structure, antiviral activity, KPG method.

INTRODUCTION

During year 2016 research on HIV-1 viruses showed great activity in all fronts (see for example [1-11]. Our Quantum Pharmacology Unit has done some research about HIV-1 inhibition by some families of chemical compounds [12-16]. To produce more knowledge concerning this subject, here we present that results of a theoretical study searching for relationships between electronic structure and HIV-1 inhibitory capacity of a group of pyrazine-1,3-thiazine hybrid analogues. There is a second important goal. Up to this date we have calculated the electronic structure of many different molecular systems with the same quantum-chemical method (B3LYP/6-31G(d,p), collecting information about the values of local atomic reactivity indices of more than 100,000 atoms. This information will be used to carry out a research for the possible creation of a database of values to be used for a first screening of molecules avoiding the quantum chemical calculations.

MATERIALS AND METHODS

The technique for finding the relationships between electronic structure and inhibition constants is now a standard one used in our Unit. We refer the reader to [17-21] and references therein. The linear system of equations to be solved has the form:

$$\log(\mathrm{BA}) = a + \sum_j \left[e_j Q_j + f_j S_j^E + s_j S_j^N \right] +$$
$$+ \sum_j \sum_m \left[h_j(m) F_j(m) + x_j(m) S_j^E(m) \right] + \sum_j \sum_{m'} \left[r_j(m') F_j(m') + t_j(m') S_j^N(m') \right] +$$

$$+\sum_j \left[g_j \mu_j + k_j \eta_j + o_j \omega_j + z_j \varsigma_j + w_j Q_j^{\max} \right] + \sum_{B=1}^{W} O_B \quad (1)$$

The local atomic reactivity indices appearing in Eq. 1 have been discussed in several publications (see for example [20, 21]. Therefore, we shall discuss below only those indices appearing in the Results section. This model-based method [22] has shown its power when applied to very different classes of molecules and biological activities (see [12, 13, 23-32] and references therein). The selected molecules are shown in Fig. 1 and Table 1 [33]. The biological activity analyzed here is the percentage of inhibition of the replication of TZM-bl cells infected with the HIV-1 NL-4.3 virus.

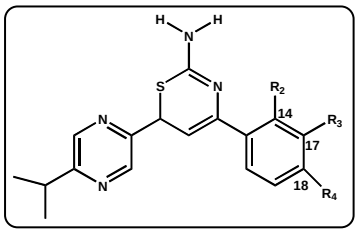

Figure 1. Pyrazine-1,3-thiazine hybrid analogues

Table 1. Pyrazine-1,3-thiazine hybrid analogues and inhibitory activity

Mol.	R_2	R_3	R_4	log(I) HIV-1
1	H	H	H	1.08
2	H	H	OMe	1.46
3	H	OMe	H	1.38
4	OMe	H	H	1.23
5	H	H	Me	1.36
6	H	Me	H	1.40
7	Me	H	H	1.45
8	H	H	OH	1.74
9	H	OH	H	1.71
10	OH	H	H	1.72
11	H	H	NO_2	1.97
12	H	NO_2	H	1.93
13	NO_2	H	H	1.92
14	H	H	Cl	1.84
15	H	Cl	H	1.81
16	Cl	H	H	1.83
17	H	H	F	1.90
18	H	F	H	1.87
19	F	H	H	1.85

Full geometry optimization and single point calculations were carried out with the Gaussian suite of programs [34]. From these results the values of the LARIs were obtained with the D-CENT-QSAR software. Mulliken Population Analysis results were corrected to avoid negative electron populations or MO populations greater than 2 [35, 36]. Keeping in mind that it is not possible to solve the system of linear equations because we have not enough molecules, we employed Linear Multiple Regression Analysis (LMRA) to find those LARIs whose variation is responsible of the variation of the inhibitory activity. For the LMRA, we built a matrix containing the logarithm of the dependent variable (log(I)), the LARIs of the atoms of the common skeleton as the independent variables The Statistica software was used [37]. The common skeleton is shown in Fig. 2.

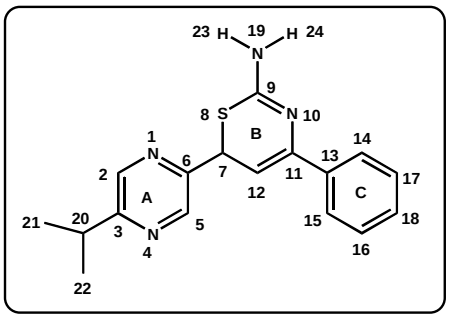

Figure 2. Common skeleton numbering

RESULTS

The best equation obtained is:

$$\log(I)=1.90+0.11S_2^N(\text{LUMO+2})^*-0.82S_3^E(\text{HOMO-1})^*-7.31S_{24}^E(\text{HOMO-2})^*+$$
$$+25.21F_{20}(\text{HOMO-2})^*+0.91S_{12}^E(\text{HOMO-2})^*+6.59F_{23}(\text{HOMO})^*+$$
$$+0.31F_4(\text{HOMO-2})^* \quad (2)$$

with n=19, R=0.98, R^2=0.96, adj-R^2=0.94, F(7,11)=42.36 (p<0.000001) and a Std. error of estimate of 0.07. No outliers were detected and no residuals fall outside the ±2σ limits. Here, S_2^N(LUMO+2)* is the nucleophilic superdelocalizability of the third lowest empty MO localized on atom 2, S_3^E(HOMO-1)* is the electrophilic superdelocalizability of the second highest MO localized on atom 3, S_{24}^E(HOMO-2)* is the electrophilic superdelocalizability of the third highest MO localized on atom 24, F_{20}(HOMO-2)* is the Fukui index (the electron population) of the third highest occupied MO localized on atom 20, S_{12}^E(HOMO-2)* is the electrophilic superdelocalizability of the third highest occupied MO localized on atom 12, F_{23}(HOMO)* is the Fukui index of the highest occupied MO localized on atom 23 and F_4(HOMO-2)* is the Fukui index of the third highest occupied MO localized on atom 4. Tables 2 and 3 show the beta coefficients, the results of the t-test for significance of coefficients and the matrix of squared correlation coefficients for the variables of Eq. 2. There are no significant internal correlations between independent variables (Table 3). Figure 3 displays the plot of observed *vs.* calculated log(I).

Table 2. Beta coefficients and t-test for significance of coefficients in Eq. 2

Variable	Beta	t(11)	p-level
S_2^N(LUMO+2)*	1.03	15.59	<0.000001
S_3^E(HOMO-1)*	-0.55	-6.73	<0.00003
S_{24}^E(HOMO-2)*	-0.34	-4.62	<0.0007
F_{20}(HOMO-2)*	0.46	5.91	<0.0001
S_{12}^E(HOMO-2)*	0.32	4.41	<0.001
F_{23}(HOMO)*	0.21	3.21	<0.008
F_4(HOMO-2)*	0.15	2.37	<0.04

Table 3. Matrix of squared correlation coefficients for the variables in Eq. 2

	S_2^N(LUMO+2)*	**S_3^E(HOMO-1)***	**S_{24}^E(HOMO-2)***	**F_{20}(HOMO-2)***	**S_{12}^E(HOMO-2)***	**F_{23}(HOMO)***
S_3^E(HOMO-1)*	**0.00**	**1**				
S_{24}^E(HOMO-2)*	**0.06**	**0.10**	**1**			
F_{20}(HOMO-2)*	**0.03**	**0.19**	**0.02**	**1**		
S_{12}^E(HOMO-2)*	**0.04**	**0.01**	**0.18**	**0.19**	**1**	
F_{23}(HOMO)*	**0.08**	**0.08**	**0.01**	**0.00**	**0.03**	**1**
F_4(HOMO-2)*	**0.00**	**0.14**	**0.01**	**0.04**	**0.02**	**0.00**

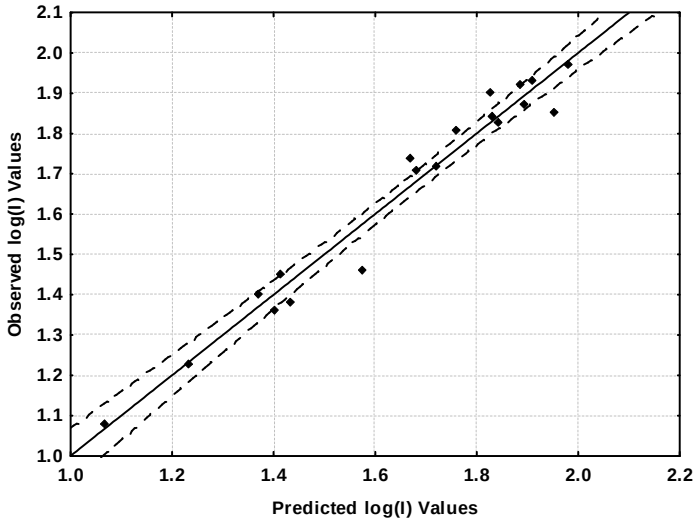

Figure 3. Plot of predicted *vs.* observed log(I) values (Eq. 2). Dashed lines denote the 95% confidence interval

The associated statistical parameters of Eq. 2 indicate that this equation is statistically significant and that the variation of the numerical values of a group of seven local atomic reactivity indices of atoms of the common skeleton explains about 94% of the variation of log(I). Figure 3, spanning about 0.9 orders of magnitude, shows that there is a good correlation of observed *versus* calculated values.

Local Molecular Orbitals

Tables 4 and 5 show the local MO structure of atoms involved in Eq. 2. Nomenclature: Molecule (HOMO) / (HOMO-2)* (HOMO-1)* (HOMO)* - (LUMO)* (LUMO+1)* (LUMO+2)*.

Table 4. Local molecular orbitals of atoms 2, 3, 4 and 12

Mol.	Mol.	Atom 2	Atom 3	Atom 4	Atom 12
1(82)	3a	80σ81σ82σ-83π84π85π	79σ80σ81σ-83π85π87π	80σ81σ82σ-83π84π87π	77σ79σ82π-83π 84π85π
2(90)	3b	85π86π88σ-91π92π93π	85π86π88σ-91π92π93π	88σ89σ90σ-91π92π95π	88π89π90π-91π92π93π
3(90)	3c	86π87σ88σ-91π92π93π	86π87σ88σ-91π92π93π	88σ89σ90σ-91π92π95π	87π89π90π-91π92π93π
4(90)	3d	86π87σ88σ-91π92π93π	86π87σ88σ-91π92π93π	87σ88σ90σ-91π92π93π	88π89π90π-91π92π93π
5(86)	3e	84σ85σ86σ-87π88π89π	83σ84σ85σ-87π88π89π	84σ85σ86σ-87π88π91π	83π85σ86π-87π88π89π
6(86)	3f	83σ84σ86σ-87π88π89π	82π83σ84σ-87π88π89π	84σ85σ86σ-87π88π91π	83π85π86π-87π88π89π
7(86)	3g	83σ84σ86σ-87π88π89π	82π83σ84σ-87π88π 89π	84σ85σ86σ-87π88π 89π	83π85σ86π-87π88π89π
8(86)	3h	81π82π84σ-87π88π89π	81π82π84σ-87π88π89π	84σ85σ86σ-87π88π91π	84π85π86π-87π88π89π
9(86)	3i	82π83σ84σ-87π88π89π	82π83σ84σ-87π88π89π	84σ85σ86σ-87π88π91π	83π85π86π-87π88π89π
10(86)	3j	83σ84σ86σ-87π88π89π	82π83σ84σ-87π88π89π	83σ84σ86σ-87π88π89π	84π85π86π-87π88π89π
11(93)	3k	91σ92σ93σ-95π96π97π	90π91σ92σ-95π96π97π	91σ92σ93σ-95π96π100π	90σ92π93π-94π95π96π
12(93)	3l	91σ92σ93σ-95π96π97π	90π91σ92σ-95π96π97π	91σ92σ93σ-95π96π97π	90σ92π93π-94π95π96π
13(93)	3m	91π92σ93σ-95π96π97π	90π91π92σ-95π96π97π	91π92σ93σ-95π96π97π	90σ92π93π-94π95π96π
14(90)	3n	88σ89σ90σ-91π92π93π	87π88σ89σ-91π93π95π	88σ89σ90σ-91π92π93π	86σ88π90π-91π92π93π
15(90)	3o	88σ89σ90σ-91π92π93π	87σ88σ89σ-91π93π95π	88σ89σ90σ-91π92π93π	85σ88π90π-91π92π93π
16(90)	3p	88σ89σ90σ-91π92π93π	87π88σ89σ-91π92π93π	88σ89σ90σ-91π92π96π	86σ88π90π-91π92π93π
17(86)	3q	84σ85σ86σ-87π88π89π	83π84σ85σ-87π89π91π	84σ85σ86σ-87π88π91π	82σ84π86π-87π88π89π
18(86)	3r	84σ85σ86σ-87π88π89π	83σ84σ85σ-87π89π90π	84σ85σ86σ-87π88π91π	83π84π86π-87π88π89π
19(86)	3s	84σ85σ86σ-87π88π89π	83π84σ85σ-87π88π89π	84σ85σ86σ-87π88π92π	82σ84π86π-87π88π89π

Table 5. Local molecular orbitals of atoms 20, 23 and 24

	Mol.	Atom 20	Atom 23	Atom 24
1(82)	3a	78σ79σ80σ-83σ95σ96σ	50σ52σ53σ-87σ88σ89σ	63σ64σ77σ-89σ90σ91σ
2(90)	3b	84σ86σ88σ-91σ104σ105σ	55σ56σ59σ-95σ96σ97σ	61σ70σ85σ-97σ98σ99σ
3(90)	3c	84σ86σ87σ-91σ104σ105σ	53σ54σ60σ-94σ95σ96σ	70σ84σ85σ-97σ98σ99σ
4(90)	3d	86σ87σ88σ-91σ104σ105σ	55σ57σ60σ-92σ94σ96σ	70σ71σ85σ-97σ98σ99σ
5(86)	3e	82σ83σ84σ-87σ99σ100σ	50σ52σ54σ-91σ92σ93σ	57σ66σ81σ-93σ94σ95σ
6(86)	3f	80σ82σ83σ-87σ99σ100σ	50σ52σ54σ-91σ92σ93σ	66σ67σ81σ-93σ94σ95σ
7(86)	3g	82σ83σ84σ-87σ99σ101σ	52σ55σ56σ-88σ90σ92σ	66σ67σ81σ-93σ94σ95σ
8(86)	3h	80σ82σ84σ-87σ100σ101σ	51σ53σ54σ-91σ92σ93σ	61σ67σ81σ-93σ94σ95σ
9(86)	3i	82σ83σ84σ-87σ100σ101σ	52σ55σ57σ-90σ91σ92σ	67σ80σ81σ-93σ94σ95σ
10(86)	3j	80σ83σ84σ-87σ99σ100σ	52σ53σ57σ-88σ90σ92σ	67σ69σ81σ-93σ94σ95σ
11(93)	3k	90σ91σ92σ-95σ107σ108σ	57σ59σ60σ-96σ99σ100σ	70σ72σ87σ-101σ102σ103σ
12(93)	3l	90σ91σ92σ-95σ107σ108σ	57σ61σ63σ-98σ99σ100σ	65σ70σ72σ-101σ102σ103σ
13(93)	3m	90σ91σ92σ-95σ107σ108σ	59σ61σ63σ-95σ99σ100σ	70σ72σ87σ-101σ102σ103σ
14(90)	3n	84σ87σ88σ-91σ103σ104σ	56σ58σ61σ-95σ96σ98σ	70σ84σ85σ-98σ99σ100σ
15(90)	3o	87σ88σ89σ-91σ103σ104σ	55σ56σ58σ-95σ96σ98σ	62σ70σ84σ-98σ99σ100σ
16(90)	3p	84σ87σ88σ-91σ104σ105σ	58σ60σ70σ-92σ95σ96σ	66σ70σ86σ-98σ99σ100σ
17(86)	3q	80σ83σ84σ-87σ99σ100σ	53σ56σ58σ-91σ92σ93σ	67σ80σ81σ-93σ94σ95σ
18(86)	3r	82σ83σ84σ-87σ99σ100σ	52σ53σ57σ-90σ91σ92σ	67σ80σ81σ-93σ94σ95σ
19(86)	3s	80σ83σ84σ-87σ99σ100σ	52σ53σ57σ-90σ91σ92σ	67σ69σ81σ-93σ94σ95σ

DISCUSSION

Equation 2 shows that there is a linear relationship between the variation of the biological property (log(I)) and the variation of the numerical values of a set of local atomic reactivity indices. Before the analysis some words are appropriate. No clear mechanism for inhibition is known. Our previous studies about HIV inhibition [12, 14-16] also obtained equations with several variables strongly suggesting that, if the inhibitory process is the result of more than one process, all the molecules seem to undergo through all of them. Note also that, despite the fact that the substitutions are in ring C, no local reactivity index of this ring appear in Eq. 1. Table 2 shows that the importance of variables in Eq. 1 is S_2^N(LUMO+2)*> S_3^E(HOMO-1)*> F_{20}(HOMO-2)*> S_{24}^E(HOMO-2)*> S_{12}^E(HOMO-2)*> F_{23}(HOMO)*> F_4(HOMO-2)*. The analysis of Eq. 2 shows that a high inhibitory activity is associated with large negative numerical values for S_{12}^E(HOMO-2)*, with high negative values for S_3^E(HOMO-1)* and S_{24}^E(HOMO-2)*, and with large values for F_{20}(HOMO-2)*, F_{23}(HOMO)* and F_4(HOMO-2)*. If S_2^N(LUMO+2)* is positive, then a

high inhibitory activity is associated with large numerical values for this index. Atom 12 is a carbon in ring B (Fig. 2). Table 4 shows that $(HOMO)_{12}$* has a π nature in all molecules, $(HOMO-1)_{12}$* has a π nature in all molecules but three, and $(HOMO-2)_{12}$* has a σ nature in nine molecules. The fact that $(HOMO-2)_{12}$* appears in the QSAR equation implies that the two highest occupied local MOs are also involved in the interaction. Considering that a low electron donor capacity of the $(HOMO-2)_{12}$* is associated with a high inhibitory activity, we suggest that for an optimal inhibitory activity, the two highest local molecular orbitals of this atom must have a π nature and also they must correspond to the two highest occupied molecular MOs with a high electron population. The best situation is a molecule in which the electron density of $(HOMO-2)_{12}$* is close to zero. Atom 12 is then interacting with an electron-deficient center. Atom 3 is a carbon in ring A (Fig. 2). Table 4 shows that $(HOMO)_3$* has a σ nature (this seems to be a direct influence of the electronic structure of the isopropyl substituent at position 3) and $(HOMO-1)_3$* is of σ or π natures. A high inhibitory activity is associated with large negative values for $S_3^E(HOMO-1)$*. Given the nature of $(HOMO)_3$*, it is suggested that a $(HOMO-1)_3$* of a σ nature and with a high electron population is optimal and that atom 3 is engaged in σ-σ and/or σ-π interactions. Atom 24 is one of the hydrogen atoms bonded to N19 (Fig. 2). Table 5 shows that all listed MOs have a σ nature. Note that the highest occupied local MO is very far from the molecule's HOMO. A high inhibitory activity is associated with large negative values of $S_{12}^E(HOMO-2)$*. As the first two highest occupied local MO are also participating in the activity, we suggest that the requirement of large electron densities in the first three highest occupied local MOs is a strong indication that atom 24 is participating in a hydrogen bond. Atom 20 is the central carbon atom of the isopropyl substituent (Fig. 2). Table 5 shows that all MOs have a σ nature. A high inhibitory activity is associated with large values for $F_{20}(HOMO-2)$*. The plot of $F_{20}(HOMO-1)$* *vs.* log(I) (not shown here) does not show a clear trend. The plot of $F_{20}(HOMO)$* *vs.* log(I) shows an feeble trend suggesting that a high value of this index seems to be associated with a high percentage of HIV-1 inhibition. Then, it seems that atom 20 is engaged in σ-σ interactions with alkyl chains localized inside an apolar environment. Atom 23 is the other hydrogen atom bonded to N19 (Fig. 2). Table 5 shows that all listed MOs have a σ nature. Note that the highest occupied local MO is very far from the molecule's HOMO. Large values of $F_{23}(HOMO)$* are associated with a high inhibitory percentage, indicating that this atom is also engaged in a hydrogen bond. Atom 4 is a nitrogen atom in ring A (Fig. 2). Table 4 shows that $(HOMO-2)_4$*, $(HOMO-1)_4$* and $(HOMO)_4$* have a σ nature. A high inhibitory activity is associated with large values of $F_4(HOMO-2)$*. The first three empty local MOs have a π nature (Table 10). The plots of $F_4(HOMO-1)$* and $F_4(HOMO)$* indicate that a high inhibitory activity is associated with high values for these indices. This suggests that atom 4 is engaged in σ-σ and/or σ-π interactions. Interestingly, atom 4 is located close to the isopropyl substituent that also seems to have these kinds of interactions. Atom 2 is a carbon atom in ring A (Fig. 2). A high inhibitory activity is associated with large numerical values for $S_2^N(LUMO+2)$* if this index is positive. Table 4 shows that the first thee lowest vacant MOs have a π nature. Large values are obtained by shifting downwards the associated eigenvalue and making this MO more reactive. Therefore, we suggest that atom 2 is engaged in π-π interactions with an electron-rich center. All these ideas are depicted in the partial two dimensional (2D) pharmacophore shown in Fig. 4.

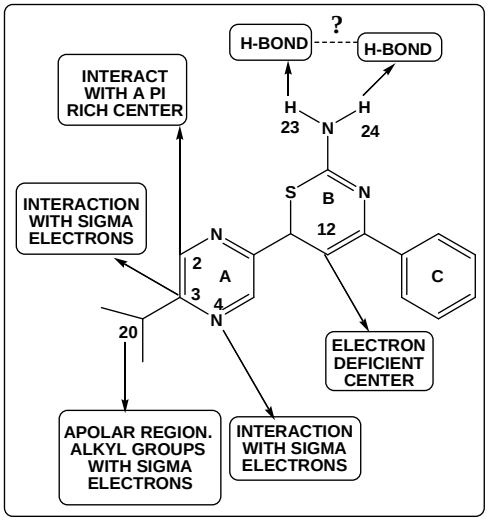

Figure 4. Partial 2D pharmacophore for the inhibition of HIV-1 by pyrazine-1,3-thiazine hybrid analogues

It is worth to mention that this is the first time in our QSAR studies that we find so many atomic centers (atoms 3, 4 and 20 in Fig. 4) with interactions pointing toward an apolar area. Only more experimental results will confirm or discard such interaction.

In conclusion, we have obtained interesting results concerning the inhibition of HIV-1 by the title molecules. No local atomic reactivity indices belonging to the substituted ring (C in Fig. 4) appeared in the results. The pharmacophore presents several atomic sites to be analyzed with different substituents. This is another example of the fact that the substitution at any atomic center may cause a modification of the electronic structure of other centers located relatively far and not connected by aromatic bridges.

REFERENCES

[1] D. Borrenberghs, L. Dirix, S. Rocha, J. Hofkens, Z. Debyser, et al., *Biophys. J.*, **2016,** 110, 647a.
[2] J. Dev, D. Park, Q. Fu, J. Chen, H. J. Ha, et al., *Science*, **2016,** 353, 172-175.
[3] J. Gorman, C. Soto, M. M. Yang, T. M. Davenport, M. Guttman, et al., *Nat Struct Mol Biol*, **2016,** 23, 81-90.
[4] J. S. Johnson, S. Lucas, S. Skelton, R. Nazitto, L. Amon, et al., *J. Immunol.*, **2016,** 196, 61.68.
[5] S. Padilla-Parra, M. L. Dustin, *Trends Mol. Med.*, **2016,** 22, 354-356.
[6] P.-J. Racine, C. Chamontin, H. de Rocquigny, S. Bernacchi, J.-C. Paillart, et al., *Sci. Rep.*, **2016,** 6, 27536.
[7] P. Rusert, R. D. Kouyos, C. Kadelka, H. Ebner, M. Schanz, et al., *Nat. Med.*, **2016,** 22, 1260-1267.
[8] F. K. M. Schur, M. Obr, W. J. H. Hagen, W. Wan, A. J. Jakobi, et al., *Science*, **2016,** 353, 506-508.
[9] Guillaume B. E. Stewart-Jones, C. Soto, T. Lemmin, G.-Y. Chuang, A. Druz, et al., *Cell*, **2016,** 165, 813-826.
[10] G. C. Todd, A. Ono, "Methods to Study Determinants for Membrane Targeting of HIV-1 Gag In Vitro," in *HIV Protocols*, V. R. Prasad, and G. V. Kalpana Eds., pp. 175-185, Springer New York, New York, NY, **2016**.
[11] I. Visan, *Nat Immunol*, **2016,** 17, 355-355.
[12] G. A. Kpotin, G. S. Atohoun, U. A. Kuevi, A. Houngue-Kpota, J.-B. Mensah, et al., *J. Chem. Pharmaceut. Res.*, **2016,** 8, 1019-1026.
[13] J. Valdebenito-Gamboa, J. S. Gómez-Jeria, *Der Pharma Chem.*, **2015,** 7, 543-555.
[14] J. S. Gómez-Jeria, M. B. Becerra-Ruiz, *Der Pharma Chem.*, **2015,** 7, 362-369.
[15] J. S. Gómez-Jeria, M. Flores-Catalán, *Canad. Chem. Trans.*, **2013,** 1, 215-237.
[16] D. A. Alarcón, F. Gatica-Díaz, J. S. Gómez-Jeria, *J. Chil. Chem. Soc.*, **2013,** 58, 1651-1659.
[17] J. S. Gómez-Jeria, *Int. J. Quant. Chem.*, **1983,** 23, 1969-1972.
[18] J. S. Gómez-Jeria, "Modeling the Drug-Receptor Interaction in Quantum Pharmacology," in *Molecules in Physics, Chemistry, and Biology*, J. Maruani Ed., vol. 4, pp. 215-231, Springer Netherlands, **1989**.
[19] J. S. Gómez-Jeria, M. Ojeda-Vergara, *J. Chil. Chem. Soc.*, **2003,** 48, 119-124.
[20] J. S. Gómez-Jeria, *Elements of Molecular Electronic Pharmacology (in Spanish)*, Ediciones Sokar, Santiago de Chile, **2013**.
[21] J. S. Gómez-Jeria, *Canad. Chem. Trans.*, **2013,** 1, 25-55.
[22] Y. C. Martin, *Quantitative drug design: a critical introduction*, M. Dekker, New York, 1978.
[23] A. Robles-Navarro, J. S. Gómez-Jeria, *Der Pharma Chem.*, **2016,** 8, 417-440.
[24] J. S. Gómez-Jeria, Í. Orellana, *Der Pharma Chem.*, **2016,** 8, 476-487.
[25] J. S. Gómez-Jeria, C. Moreno-Rojas, *Der Pharma Chem.*, **2016,** 8, 475-482.
[26] J. S. Gómez-Jeria, M. Matus-Perez, *Der Pharma Chem.*, **2016,** 8, 1-11.
[27] J. S. Gómez-Jeria, V. Gazzano, *Der Pharma Chem.*, **2016,** 8, 21-27.
[28] J. S. Gómez-Jeria, R. Cornejo-Martínez, *Der Pharma Chem.*, **2016,** 8, 329-337.
[29] J. S. Gómez-Jeria, H. R. Bravo, *Der Pharma Chem.*, **2016,** 8, 25-34.
[30] J. S. Gómez-Jeria, S. Abarca-Martínez, *Der Pharma Chem.*, **2016,** 8, 507-526.
[31] H. R. Bravo, B. E. Weiss-López, J. Valdebenito-Gamboa, J. S. Gómez-Jeria, *Res. J. Pharmac. Biol. Chem. Sci.*, **2016,** 7, 792-798.
[32] M. S. Leal, A. Robles-Navarro, J. S. Gómez-Jeria, *Der Pharm. Lett.*, **2015,** 7, 54-66.
[33] H.-M. Wu, K. Zhou, T. Wu, Y.-G. Cao, *Chem. Biol. Drug Des.*, **2016,** 88, 411-421.
[34] M. J. Frisch, G. W. Trucks, H. B. Schlegel, G. E. Scuseria, M. A. Robb, et al., G03 Rev. E.01, Gaussian, Pittsburgh, PA, USA, **2007**.
[35] J. S. Gómez-Jeria, D-Cent-QSAR: A program to generate Local Atomic Reactivity Indices from Gaussian 03 log files. v. 1.0, Santiago, Chile, **2014**.
[36] J. S. Gómez-Jeria, *J. Chil. Chem. Soc.*, **2009,** 54, 482-485.
[37] Statsoft, Statistica v. 8.0, 2300 East 14 th St. Tulsa, OK 74104, USA, **1984-2007**.